Research Article

Wei Dong and Yajing Ji*

Chloride ion transport and service life prediction of aeolian sand concrete under dry–wet cycles

https://doi.org/10.1515/secm-2022-0188
received October 19, 2022; accepted February 12, 2023

Abstract: In this study, the dry–wet cycle test of chloride salt was carried out on aeolian sand concrete with different contents, and the chloride ion content in aeolian sand concrete was determined by taking powder from different depths on one side of the test block. And then combined with Monte Carlo stochastic statistical simulation and Weibull probability distribution function, the service life prediction model of aeolian sand concrete against chloride ion erosion is established. The results show that the free chloride ion content in aeolian sand concrete decreases with the increase in the depth from the surface of the specimen. At the same depth from the surface of the specimen, the free chloride ion content gradually increases with the increase in the number of dry–wet cycles. Through the analysis of life prediction, it is concluded that with the increase in aeolian sand content, the service life of aeolian sand concrete increases first and then decreases. The service life value of concrete with 75% aeolian sand content is the largest, and the greater the thickness of the protective layer, the more favorable the service life value.

Keywords: aeolian sand concrete, chlorine salt dry–wet cycles, durability, chloride ions erosion, service life prediction

1 Introduction

Concrete is a widely used artificial stone, and as its consumption increases year by year, the lack of concrete raw material resources is gradually highlighted [1,2]. Regarding natural resources, China began to strengthen the environmental protection. Northern and northwestern China have abundant desert resources, and aeolian sand often erodes roads and fertile farmland there, which seriously damages the natural environment and causes major economic losses [3,4]. Today, it is advocated that "lucid waters and lush mountains are invaluable assets." If the aeolian sand resources can be rationally utilized, it cannot only curb land desertification and protect the natural environment, but also reduce the collection and transportation costs of engineering sand [5].

Due to the particle characteristics of aeolian sand, different content of aeolian sand can change the functional properties of concrete. Several scholars [6–9] studied the engineering characteristics of aeolian sand and aeolian sand concrete. Yan et al. [10] provided an optimization design method for desert sand concrete mixture ratio based on a statistical model. Dong et al. [11] studied the freeze-thaw cycle of aeolian sand lightweight aggregate concrete and found that the optimal replacement rate of aeolian sand is 20%. Al-Harthy et al. [12] has shown that aeolian sand as a fine aggregate can change the workability of concrete. With the increase in aeolian sand content, the slump of concrete increases. Through the study of aeolian sand concrete, Abu Seif et al. [13] found that aeolian sand concrete can be used for normal reinforcement work, with no vibration and effect of no vibration and heavy vibration. Wu et al. [14] studied the carbonation performance of aeolian sand concrete and established a carbonation life prediction model. The research shows that aeolian sand can improve the carbonation resistance of concrete, and the increase is most obvious when the content is 60%. Besides, Luo et al. [15] found that when the sand–cement mass ratio is greater than 1.41, the workability of aeolian sand concrete is not significantly different from that of ordinary concrete. Although there are many studies on aeolian sand concrete, the application research on aeolian sand concrete mainly focuses on its macroscopic working performance, mechanical properties, and damage performance under freeze-thaw conditions, while there are few studies on chloride salt erosion, which is now more valued.

The destruction of chlorine and salt erosion on the concrete structure is increasingly valued by experts and scholars, especially the concrete structure in the dry–wet

* **Corresponding author: Yajing Ji,** School of Civil Engineering, Inner Mongolia University of Science and Technology, Baotou 014010, China, e-mail: 970096105@qq.com
Wei Dong: College of Civil Engineering, Inner Mongolia University of Science and Technology, Baotou 014010, China

alternation region [16–18]. Salt lakes, coastal cities, and urban roads and bridges that are eroded with ice and salt are often rusted by various erosive ions, thus resulting in concrete structure service failure. Many researchers have explored the transmission mechanism of chloride ions in cement-based materials and used this to predict the service life of cement-based materials in chlorine and salt erosion, thereby achieving many research results. Liu et al. [19] proposed that the diffusion of chloride ions in concrete can be described by Fick's law of diffusion when the concrete is an isotropic homogeneous material and the chloride ions that penetrate the concrete do not react with the hydration products under ideal conditions. Mangat and Molloy [20] studied the influence of aging on the concrete Cl-diffusion coefficient and established a modified model when the chloride diffusion coefficient is in the form of a power function. Many scholars [21–23] have considered the influence of various factors such as the concrete surface environment on the binding chloride ion and chloride ion diffusion coefficient and obtained the service life prediction model of the concrete structure. Yu et al. [24] derived a modified model of concrete chloride ion diffusion theory considering the action of various factors based on Fick's second law and gave analytical solutions for the one-, two-, and three-dimensional cases. Kang et al. [25] studied the chloride ion transport properties in fiber-recycled concrete under the action of dry–wet cycles. Their results showed that the free chloride ion content first increases, then decreases with the increase in sampling depth after the action of dry–wet cycles, and the incorporation of fiber can improve the chloride ion erosion resistance of concrete. An et al. [26] established a prediction model for the service life of concrete structures against chloride ion erosion damage by combining Monte Carlo random simulation with Weibull distribution function through the durability of reactive powder concrete under seawater freeze-thaw action. In summary, the transport and life prediction model of concrete chloride ions under the action of dry–wet cycles have obtained certain research results, yet the current life prediction model parameters are not highly diversified, and there has been less research on the life prediction of aeolian sand concrete. Based on this, this study investigates the variation law of chloride ion content in concrete under the action of dry–wet cycles of chloride salts, with different aeolian sand admixtures and at different depths, and predicts the service life of aeolian sand concrete under the action of chloride ion erosion.

2 Experimental program

2.1 Materials and methods

P·O 42.5 Portland cement produced by Inner Mongolia Mengxi Cement Co. Ltd was used in this study. Fly ash was selected from grade II fly ash of the Daqi power plant in Inner Mongolia. The basic physical properties of fly ash are shown in Table 1. Common river sand and aeolian sand as fine aggregate were used to prepare the aeolian sand concrete. Common river sand was taken from sand factories near Baotou City. Aeolian sand was taken from the middle of the Ordos Desert in Inner Mongolia, and the main particle size was 0.075–0.25 mm. The main physical properties of the fine aggregates are shown in Table 2. The particle size distribution curve is shown in Figure 1. The coarse aggregate was 5–25 mm continuously graded common gravel. The apparent density was 2,580 kg/m^3, bulk density was 1,610 kg/m^3, with a mud content of 2.5%, crushing index of 3.9%, and water content of 0.2%. The water was ordinary tap water from Baotou City. The additive was a polycarboxylic acid composite high-efficiency water-reducing and air-entraining agent with a 23% water reduction rate.

2.2 Experimental matching ratio and method

The concrete mix ratio design adopted in this test refers to the "Ordinary concrete mix ratio design procedure" (JGJ55-2011) [27]. Aggregate specifications were selected according to the "standard for sand and stone quality and inspection methods for ordinary concrete" (JGJ52-2006) [28]. The strength grade of the C30 ordinary concrete matching ratio was used as the reference group, and 10% fly ash was added to replace cement to ensure that

Table 1: Basic physical properties of fly ash

45 μm fineness (%)	Water requirement (%)	Loss on ignition (%)	Moisture content (%)	Density (kg/m^3)	Bead content (%)
18	100	6.5	1.0	2,435	94.0

Table 2: Main physical performance indexes of fine aggregate

Type	Apparent density (kg/m³)	Bulk density (kg/m³)	Mud content (%)	Moisture content (%)	Fineness modulus	Chloride ion content (%)
River sand	2,610	1,550	0.9	2.0	2.6	0.25
Aeolian sand	2,660	1,570	0.3	0.2	0.8	0.02

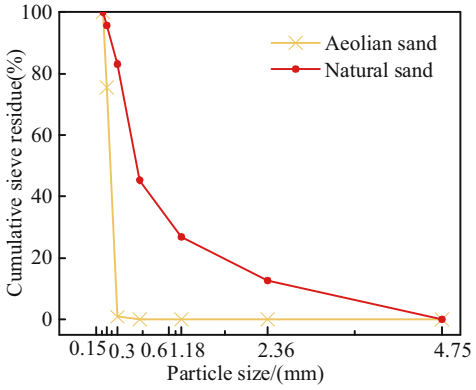

Figure 1: Aeolian sand and river sand particle size distribution.

the slump was ≥120 mm. The admixture was 1% of cementitious material, the sand rate was 0.42, and the water-cement ratio was 0.55. The aeolian sand was prepared by replacing the ordinary river sand of equal quality with aeolian sand of mass ratios of 0, 25, 50, 75, and 100%, as shown in Table 3.

The preparation of concrete is based on the "Ordinary concrete mixture performance test method standard" (GB/T50080-2016) [29]. A forced mixer was used to mix the aeolian sand concrete, then the concrete mixture was injected into the test mold, and covered with plastic wrap to prevent the moisture of the test mold concrete from evaporating. The mixture was then cured for 28 days in a standard curing room with (20 ± 2)°C and humidity above 95%. According to the relevant norms and standards [30], the artificial simulated dry–wet cycles test was carried out. The test adopts a cycle of 4 days (dry–wet ratio of 1:3), and a dry–wet cycle test for a period of 100 days. The chloride ion concentration was measured using a 100 mm × 100 mm × 100 mm cube. When the concrete specimen was cured for 26 days, the specimen was removed, the moisture on the surface of the specimen was wiped off, and then it was placed in a drying oven at (80 ± 5)°C for 2 days. Next it was placed in a 3.5% NaCl (mass concentration) solution for 3 days, then it was removed, its surface was wiped, and it was placed in a drying box to dry for 1 day, which is counted as a dry–wet cycle. When the dry–wet cycle was 0, 5, 10, 15, 20, and 25 times, drill holes were made on one side of the test block to collect powder, and the drilling depths were (0–5), (5–10), (10–15), (15–20), and (20–25) mm, the experiment refers to "Technical Specifications for Testing and Testing of Concrete in Water Transport Engineering" (JTS/T 236-2019) [31] to measure the chloride ion concentration in concrete powder and record the relevant data.

3 Experimental results

3.1 Influence of dry–wet cycles times on free chloride ion content

Figure 2 shows the regular curves of the change in free chloride ion content with the amount of aeolian sand at different depths from the surface of the concrete in the

Table 3: Mixture ratio of aeolian sand concrete (kg/m³)

Group	Cement	Fly ash	River sand	Aeolian sand	Coarse aggregate	Water	Admixture
A0	297	33	800	0	1,090	180	3.3
A25	297	33	600	200	1,090	180	3.3
A50	297	33	400	400	1,090	180	3.3
A75	297	33	200	600	1,090	180	3.3
A100	297	33	0	800	1,090	180	3.3

Note: For example, A50 represents the concrete with 50% of aeolian sand.

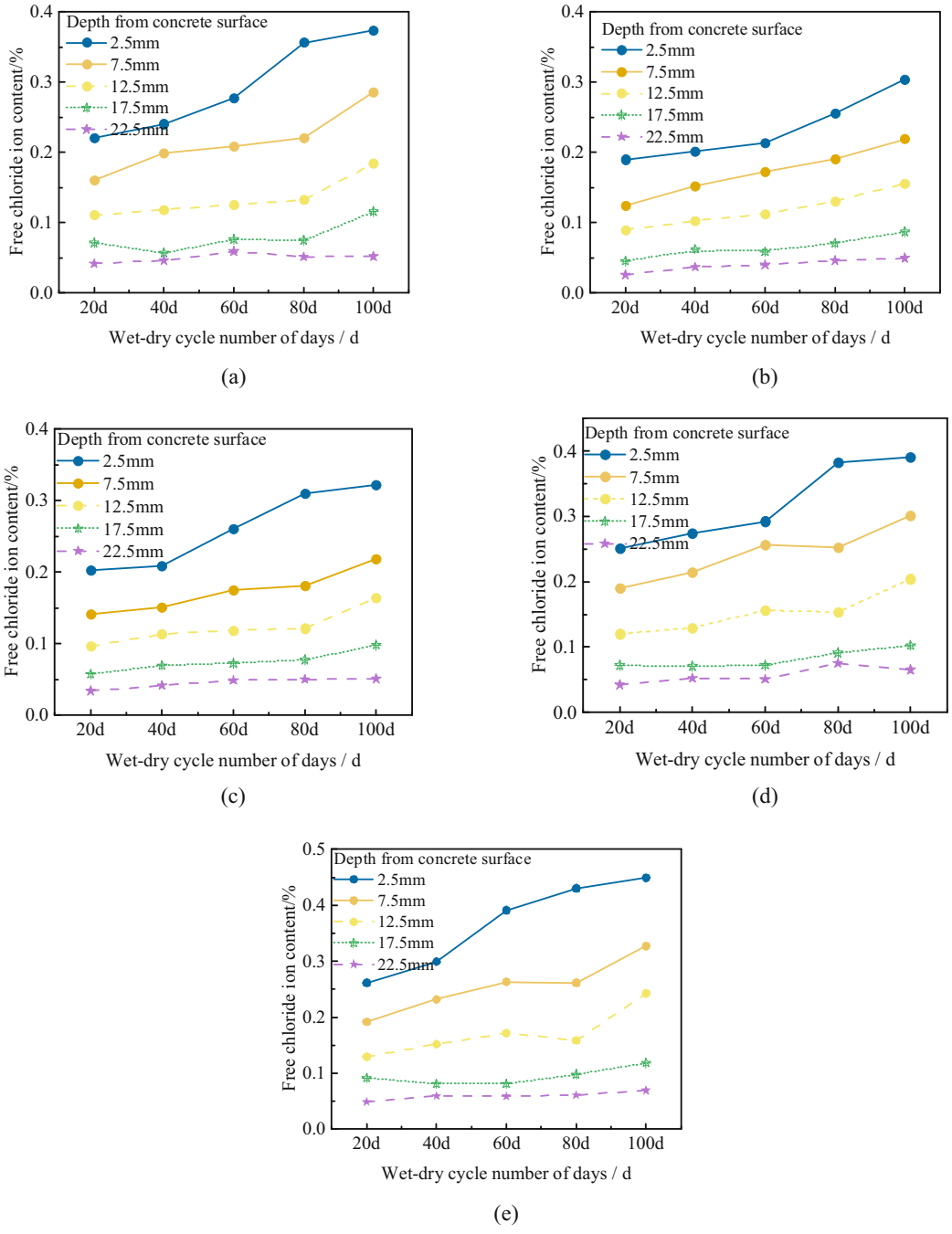

Figure 2: Free chloride ion content on different dry–wet cycles. (a) A0, (b) A25, (c) A50, (d) A75, and (e) A100.

concrete under the action of the dry–wet cycles. It can be seen from Figure 2 that, with the increase in the number of dry–wet cycles, the content of free chloride ions at the same depth increases with the number of dry–wet cycles, and the increase is most obvious between 0-5 mm on the concrete surface. In order to facilitate the representation, the intermediate value of each borehole depth is selected for drawing. In addition, with the increase in depth, the increase in free chloride ion content showed a downward trend. During the dry–wet cycles, the concrete specimen often comes into contact with the salt solution in an unsaturated state. The solution is adsorbed by the open pores in the concrete surface through capillary absorption, and then the chloride ions gradually diffuse into the concrete through the concentration gradient. When the surrounding environment is dry, the water in the

open pores of the concrete gradually evaporates to the outside, until the internal humidity and the external environmental humidity reach a balance. However, during the migration process, due to the viscous resistance of the concrete pore walls and the inherent "ink bottle-bundle tube" shape of the concrete pore structure [32], chloride ions will accumulate on the surface of the concrete. This will gradually form a salt-supersaturated solution and salt crystals will be precipitated. The continuous accumulation and expansion of crystals will first cause damage to the concrete surface, in turn causing the dry–wet cycles to have a greater impact on the free chloride ions on the concrete surface.

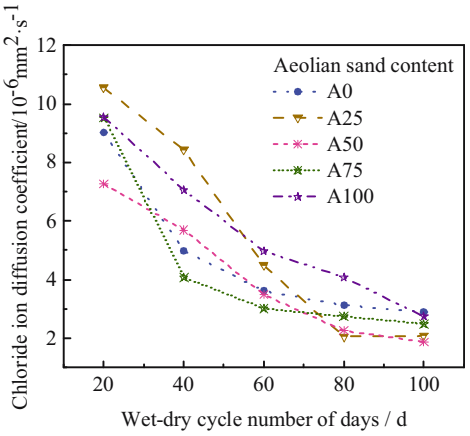

Figure 3: Spline curve diagram of chloride ion diffusion coefficient.

3.2 Concrete chloride diffusion coefficient

Aeolian sand concrete is a porous cement-based material, and the diffusion of chloride ions in it obeys Fick's second law, the analytical solution is as follows [19]:

$$C(x, t) = C_0 + (C_s - C_0)\left[1 - \text{erf}\frac{x}{2\sqrt{Dt}}\right], \quad (1)$$

where t represents the diffusion time, s and x represents the depth from the concrete surface, mm. D represents the chloride ion diffusion coefficient, mm^2/s. C represents the chloride ion concentration, which is a function based on x and time t, %. C_s represents the surface chloride ion concentration, %. C_0 represents the initial chloride ion content of the concrete, %. And the erf is the Gaussian error function.

Based on the measured concentration of chloride ions in the diffusion zone of concrete at different depths of the test, the value of chloride ion diffusion coefficient D for concrete with a different number of wet–dry cycles can be obtained according to equation (1). Figure 3 shows the line chart of the variation in chloride diffusion coefficient for each group of concrete. It can be seen from the curve trend in Figure 3 that with the continuous dry–wet cycles of concrete, the chloride ion diffusion coefficients show a decreasing trend with the increase in dry–wet cycles. The reason for the above analysis results are as follows: Aeolian sand bleeds into the concrete, resulting in the existence of many small internal pores [4].

To study the mechanism of chloride ion on aeolian sand concrete more completely, the nuclear magnetic resonance pore structure analysis test of aeolian sand concrete was carried out [33]. The test showed that the addition of aeolian sand had a great influence on the internal pores of the concrete. When the amount of aeolian sand is 25%, the peak points of the T_2 spectrum curve of the concrete show a significant decrease compared with the A0 benchmark group. And the pore size of A100 group concrete increases obviously. A small amount of aeolian sand is incorporated into the concrete, which has a positive effect on the dense concrete. With the increase in the amount of aeolian sand, the excess pore structure inside the concrete begins to increase. In the dry–wet cycles, in the early stage, the water and chloride ions intrusion are greater, with the surrounding environment of dry water gradually evaporating to the outside. Furthermore, due to the existence of the pore wall on its "retention" effect, most chloride ions remain in the concrete pores. This was obtained by the electron microscope test of aeolian sand concrete in the study by Iv [3]. Aeolian sand and cement stone are closely wrapped in one. There are a large number of network C–S–H gels and the precipitated needle-like AFt crystals are filled between the pores. The two are closely intertwined to build a stable overall structure. As the dry–wet cycles proceed, the internal water continues to evaporate, and the excess salt solution forms a salt-saturated solution, which precipitates excess salt crystals, and is stored in the pores to block the pores and chloride ion transport channels, which in turn leads to a rapid decrease in the D value of A0 and A75 group concrete in the early stage of the dry–wet cycles. The concrete of the A25 and A50 groups with a small amount of aeolian sand admixture showed a relatively slow decreasing trend in the early stage due to fewer internal pores [4] and less water and chloride ions absorbed in the early stage, while due to the continuous dry–wet cycles, the chloride salt solution continuously invaded the concrete interior, and the gradual accumulation of salt crystals led to a rapidly decreasing trend of D value in the middle stage.

When describing chloride ion diffusion by Fick's second law, diffusion is a more steady-state diffusion

process. However, from the curves shown in Figure 3, it is clear that the D value is a temporal function, and the D value shows an exponential relationship with time. The research model is shown in equation (2) as follows [20,34]:

$$D_t = D_0\left(\frac{t_0}{t}\right)^m, \tag{2}$$

where D_0 is the chloride diffusion coefficient at time t_0, and D_t is the chloride diffusion coefficient at time t. m represents the time dependence constant.

The time dependence coefficient m of the D value is obtained by substituting the D value of each group in formula (2), as shown in Table 4.

3.3 Service life prediction of aeolian sand concrete damaged by chloride ion erosion

The chloride ion permeability performance is a key index for evaluating the durability of concrete structures in the marine environment. According to the specification "Concrete Structure Durability Design and Construction Guide," when the thickness of the protective layer of a concrete structure is more than 95% or equal to the minimum thickness of the protective layer, then the allowable deviation of the concrete protective layer is taken to be ±10 mm, and its parameters obey the normal distribution $N[X,(\triangle X/1.645)^2]$. Using equation (1) as the basis for life prediction of marine concrete, when the chloride ion concentration on the surface of the reinforcement inside the aeolian sand concrete reaches the critical chloride ion content C_{cr} for reinforcement corrosion, the concrete structure is considered to be damaged, then equation (1) can be rewritten as follows [39]:

$$t = \frac{x^2}{4D\left[\text{erf}^{-1}\left(1 - \frac{C_{cr}}{C_s}\right)\right]^2}. \tag{3}$$

To determine the value of service life t of concrete under the action of different protective layer thicknesses x, it is necessary to determine the values of each parameter (D, C_s, C_0, and C_{cr}) in the equation. According to the previous studies [35–37], C_{cr} is taken to be 0.4% and obeys a normal distribution of N[0.4%, $(0.04\%)^2$]; according to the literature [38] and equation (2), taking the coefficient of variation of chloride ion diffusion coefficient as 5.31%, the distribution of chloride ion diffusion coefficient for different admixtures of aeolian sand concrete can be obtained, as shown in Table 5. According to the literature [39], C_s was taken as 3.5% with a standard deviation of 0.8%, obeying a normal distribution N[3.5%, $(0.8\%)^2$].

During the concrete construction and service process, the material surface chloride ion content changes, non-homogeneous material concrete diffusion coefficient of chloride ions at various places also exhibit differences in the construction and placement process of water, and the material chloride ion content control is not the same, thus the molding concrete protective layer thickness cannot be very accurate. The presence of errors in each factor leads to the parameters in the service life prediction model for concrete structures being random variables, in turn requiring a probabilistic statistical analysis of each parameter. The random parameters generated by the simulated random variables are added to equation (3) to determine their lifetime values, while the lifetime values are later analyzed to determine their distribution characteristics and other characteristic quantities.

The protective layer in concrete can avoid the reinforcement from being exposed directly, thereby effectively protecting the reinforced concrete from rust damage. According to the "Concrete Structure Durability Design and Construction Guide," the minimum concrete

Table 4: Time dependence coefficient m of different contents of aeolian sand concrete

Aeolian sand content (%)	0	25	50	75	100
m	0.77	0.62	0.73	0.98	0.64

Table 5: Distribution of chloride ion diffusion coefficient of concrete with various aeolian sand contents

Group	Mean ($mm^2\,a^{-1}$)	Variance ($mm\,a^{-2}$)	Coefficient of variation (%)	Normal distribution
A0	30.39	2.605	5.31	N[30.39, 2.605]
A25	36.51	3.758	5.31	N[36.51, 3.758]
A50	27.53	2.137	5.31	N[27.53, 2.137]
A75	17.43	0.857	5.31	N[17.43, 0.857]
A100	46.97	6.220	5.31	N[46.97, 6.220]

Table 6: Distribution characteristics of each parameter

Parameter	Group	Mean ($mm^2\ a^{-1}$)	Variance ($mm\ a^{-2}$)	Coefficient of variation (%)	Normal distribution
D ($mm^2\ a^{-1}$)	A0	30.39	2.605	5.31	N[30.39, 2.604]
	A25	36.51	3.758	5.31	N[36.51, 3.758]
	A50	27.53	2.137	5.31	N[27.53, 2.137]
	A75	17.43	0.857	5.31	N[17.43, 0.857]
	A100	46.97	6.220	5.31	N[46.97, 6.221]
C_{cr} (%)		0.4	0.0016	10	N[0.4, 0.0016]
C_s (%)		3.5	0.64	22.86	N[3.5, 0.64]
X (mm)	30	30	36	20	N[30, 36]
	40	40	36	15	N[40, 36]

cover thicknesses of 30 and 40 mm of walls and beams are selected for the life prediction calculation. The distribution characteristics of the various parameters are shown in Table 6.

The Monte Carlo statistical simulation analysis method is introduced in the systematic analysis of the test data, where the frequency of events is used instead of the probability of events, and the random numbers of various parameters required for the life prediction model are generated by several thousands of Monte Carlo simulations. Then, the parameters are added to equation (3) to obtain the service life prediction values of concrete structures. The classical two-parameter Weibull distribution was obtained by fitting the Weibull distribution to the service life values generated above, and the Weibull distribution probability density function $f(t)$, cumulative distribution function $F(t)$, and its expectation $E(t)$ are as follows [39]:

$$f(t) = \frac{\beta}{\alpha} \cdot \left(\frac{t}{\alpha}\right)^{\beta-1} \cdot \exp\left[-\left(\frac{t}{\alpha}\right)\beta\right], \quad t \geq 0, \tag{4}$$

$$F(t) = 1 - \exp\left[-\left(\frac{t}{\alpha}\right)\beta\right], \tag{5}$$

$$E(t) = \alpha\gamma\left[1 + \frac{1}{\beta}\right], \tag{6}$$

where α is the scale parameter, and β is the shape parameter (α, β are greater than 0). The identity transformation of equation (5) can be obtained as follows:

$$\lg \text{ and } \lg[1 - F(t)]^{-1} = \beta \ \lg \ t - \lg\frac{\alpha^{\beta}}{\lg \ e}. \tag{7}$$

Using $y = \lg\lg[1 - F(t)]^{-1}$ as the vertical coordinate on the left side of the equation, the right side $x = \lg t$ of the equation is the horizontal coordinate, which is constant. Then, equation (7) is transformed as follows:

$$y = \beta x + b. \tag{8}$$

The Weibull distribution can be represented by transforming it into a linear distribution.

To determine whether the concrete life values comply with the Weibull distribution, the data generated by the

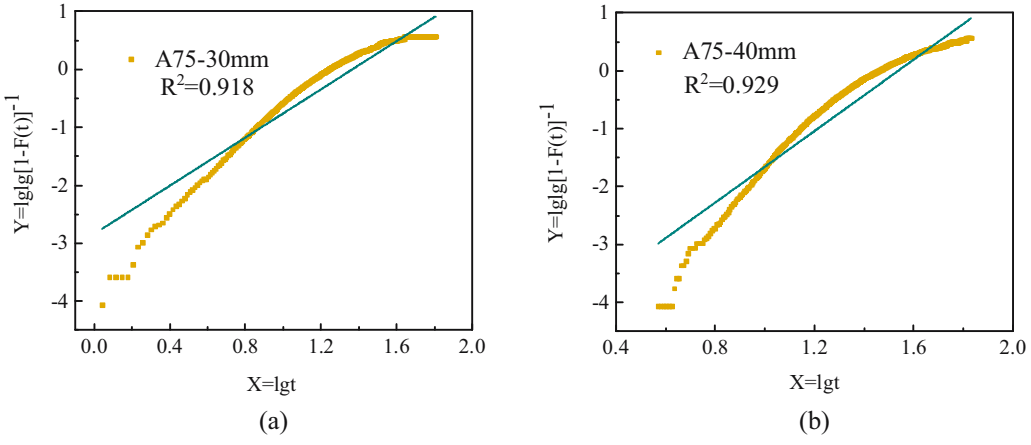

Figure 4: Weibull distribution fitting of 75% concrete with aeolian sand. (a) Protective layer thickness 30 mm. (b) Protective layer thickness 40 mm.

Table 7: Average lifetime value of each group of aeolian sand concrete under different protective layer thicknesses

Thickness of the protective layer	Group	α	β	Average life span a/min
30 mm	A0	9.68	1.43	$8.8/5.6 \times 10^7$
	A25	7.51	1.93	$6.7/4.2 \times 10^7$
	A50	10.41	1.83	$9.3/5.9 \times 10^7$
	A75	15.53	2.08	$13.8/8.7 \times 10^7$
	A100	6.15	1.43	$5.6/3.5 \times 10^7$
40 mm	A0	17.46	2.31	$15.5/9.8 \times 10^7$
	A25	12.8	2.37	$11.34/7.2 \times 10^7$
	A50	19.47	2.5	$17.3/11 \times 10^7$
	A75	26.28	3.08	$23.5/14.8 \times 10^7$
	A100	11.52	1.67	$10.3/6.5 \times 10^7$

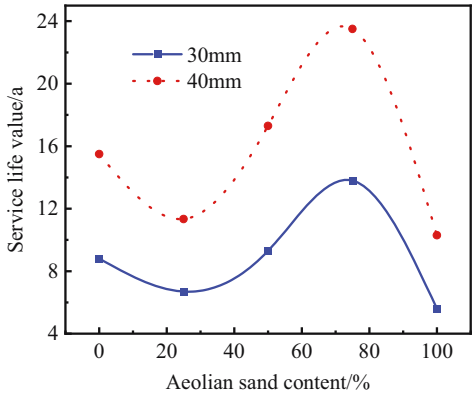

Figure 6: The life value changes with the amount of aeolian sand.

aeolian sand concrete are linearly fitted. Figure 4 shows the graph of the Weibull distribution fitted for the aeolian sand admixture with 75% concrete at the protective layer thickness of 30 and 40 mm, respectively, with the correlation coefficients R^2 of 0.918 and 0.929, respectively. From the curve situation in the graph and the size of the correlation coefficient, it can be seen from the curve situation and the magnitude of the correlation coefficient in the figure that the service life of the aeolian sand concrete better obeys the Weibull distribution.

The values of linear coefficients β and b of each group of concrete are obtained by fitting. According to the relationship between b, β, and α, the proportional parameter α of each group of concrete can be obtained, and the two parameters of Weibull distribution are obtained. The two parameters are shown in Table 7. The Weibull distribution probability density function and cumulative distribution failure probability function of each group of aeolian sand concrete can be obtained by substituting the values of parameters α and β in equations (4) and (5). Figure 5 shows the distribution probability function and cumulative distribution failure probability function of concrete with 75% aeolian sand content. It can be seen from Figure 5 that as the thickness of the protective layer increases, the probability density function shifts to the right as a whole, indicating that the service life of the concrete tends to increase. According to the cumulative distribution failure probability function of concrete under different thicknesses, the service life values of each group of concrete under specific failure probability can be obtained.

By calculating the expected value of the probability density function in equation (6), the two-parameter values are added to obtain the average service life values for each group of concrete, as shown in Table 7. From the service life values of each group of concrete in the table, it can be seen that the admixture of aeolian sand bears a significant effect on the concrete life. In the case where concrete protection layer thickness is certain, the service life of A75

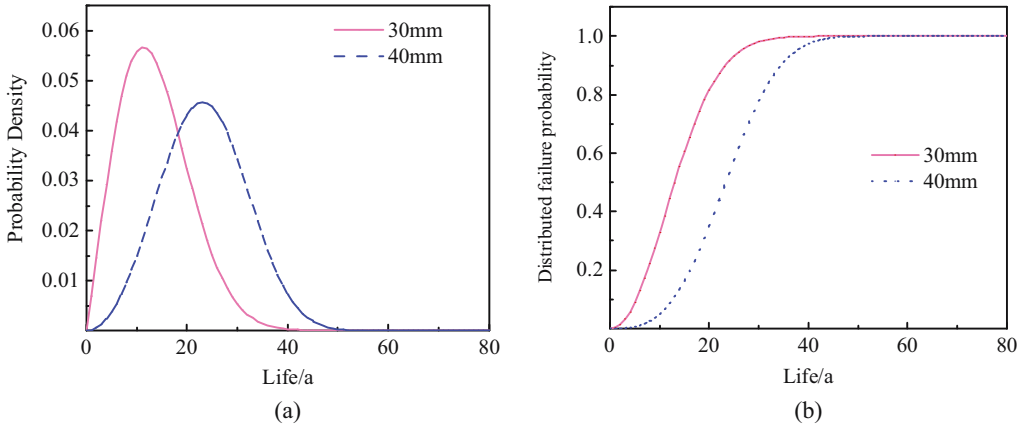

Figure 5: Weibull distribution function diagram of A75. (a) Probability density plot. (b) Cumulative distribution failure probability plot.

(concrete with 75% of aeolian sand) is the greatest, and the service life reaches the minimum value at A100 (100% of the aeolian sand).

To better visualize the effect of the amount of sand on the life of concrete at a certain thickness of the protective layer, a sample plot of the variation in the life value with the amount of sand is shown in Figure 6. As shown in Figure 6, with the change in the amount of sand, the service life of the concrete appears to first decrease, then increase, and the peak of the life value is near 75% of the sand. With the increase in the thickness of the protective layer, the difference between the two peaks gradually increases, indicating that the greater the thickness of the protective layer is, the greater the impact of the change in the amount of sand on the service life value of concrete will be. The analysis of the reason for this shows that the protective layer thickness is small, and each group of aeolian sand concrete in the chloride ions more easily enters the internal area, thus weakening the aeolian sand admixture on the concrete life value. From the curve trend in Figure 6 combined with Table 7, it can be seen that the service lifetime value of concrete can be improved with 75% of aeolian sand admixture, and that of concrete with 100% of aeolian sand admixture is most greatly reduced. The service life value of A75 is 2.28 times that of A100 and 1.52 times that of A0 when the concrete protection layer thickness is 40 mm. At 75% of aeolian sand, the protective layer thickness increased from 30 to 40 mm, and the concrete life value increased by 70.29%. This shows that one of the main ways to increase the service life of concrete structures is to increase the protective layer thickness of concrete.

4 Conclusion

In this study, five types of aeolian sand concrete with different substitution rates were tested for 100 days under the condition of drying for 1 day and wetting for 3 days. After measuring the chloride ion content at different depths of concrete, and combining Monte Carlo random statistical simulation and Weibull probability distribution function, the influence of chloride ion diffusion on the life of aeolian sand concrete structure under dry–wet cycle conditions were studied. Based on the results of this study, the following conclusions are drawn.

- Through the study of the change in free chloride ion content with the amount of aeolian sand at different depths of the surface of the concrete under the condition of the dry–wet cycles, it is found that the effect of the dry–wet cycles on different amounts of aeolian sand concrete is consistent. The free chloride ion content at the same depth from the surface of the specimen increases with the increase in the number of dry–wet cycles, and the increase in free chloride ion content decreases with the increase in depth.
- Based on the measured concentration of chloride ions in the diffusion zone of concrete at different depths of the test, the chloride ion diffusion coefficient decreases with the increase in dry and wet times as per Fick's second law. In the early stage of the dry and wet cycle, the amount of water and chloride ion intrusion is large, and the dry water of the surrounding environment evaporates to the outside, while the pore wall retains chloride ions. As the dry–wet cycle progresses, the internal water continues to evaporate, and the excess salt solution forms a saturated salt solution, which precipitates excess salt crystals and stores them in pores to block pores and chloride ion transport channels.
- Based on Monte Carlo stochastic simulation and Weibull distribution theory, a service life prediction model of aeolian sand concrete structure based on chloride ion erosion failure as the control factor is established. The analysis of the service life prediction of aeolian sand concrete shows that with the increase in aeolian sand content, the service life of aeolian sand concrete increases first and then decreases. When the thickness of the concrete cover is 30 mm, the service life of the aeolian sand concrete structure is more than 3.2×10^7 min. When the thickness of the concrete cover is 40 mm, the service life of the aeolian sand concrete structure is more than 6.3×10^7 min.

Funding information: This study was supported by the National Natural Science Foundation of China (52268044), Natural Science Foundation of Inner Mongolia Autonomous Region (2021LHMS05019), and an Open fund project of the Institute of Building Science, Inner Mongolia University of science and technology (JYSJJ-2021Q01).

Author contributions: Wei Dong was involved in methodology, conceptualization, project management, and funding acquisition, and Yajing Ji performed data collation, writing – review and editing.

Conflict of interest: The authors state no conflict of interest.

Data availability statement: All data appear in the submitted article.

References

[1] Li KF, Lian HZ, Di XT. Durability design of concrete structures: principle method and standard. China Civil Engineering Journal. 2021;54(10):64–71. doi: 10.15951/j.tmgcxb.2021.10.010.

[2] Fei TT, Jiang JY, Liu ZY. Impact compression mechanical properties of ultra-high performance concrete with manufactured sand. J Chin Chem Soc. 2020;48(08):1177–87. doi: 10.14062/j.issn.0454-5648.20200222.

[3] lv S. Effect of aeolian sand and fly ash content on mechanical properties of concrete. J Chin Chem Soc. 2018;37(7):2320–5. doi: 10.16552/j.cnki.issn1001-1625.2018.07.043.

[4] Bai JW, Zhao YR, Shi JN. Damage degradation model of aeolian sand concrete under freeze-thaw cycles based on macro-microscopic perspective. Constr Build Mater. 2022;327:126885. doi: 10.1016/j.conbuildmat.2022.126885.

[5] Dong W, Shen XD, Xue HJ. Research on the freeze-thaw cyclic test and damage model of Aeolian sand lightweight aggregate concrete. Constr Build Mater. 2016;123:792–9. doi: 10.1016/j.conbuildmat.2016.07.052.

[6] Zhang GX, Song JX, Yang J, Liu XY. Performance of mortar and concrete made with a fine aggregate of desert sand. Build Environ. 2006;41(11):1478–81. doi: 10.1016/j.buildenv.2005.05.033.

[7] Elipe M, Lopez-Querol S. Aeolian sands: Characterization, options of improvement and possible employment in construction-The State-of-the-art. Constr Build Mater. 2014;73:728–39. doi: 10.1016/j.conbuildmat.2014.10.008.

[8] Dong RX, Shen XD, Xue HJ, Wei LS, Mu R. Influence of air void parameters of aeolian sand concrete on its strength. MATREP. 2022;36(12):105–9. https://www-webofscience-com-s.webvpn.imust.edu.cn:8118/wos/alldb/full-record/CSCD:7239530.

[9] Li DB, Wang YS, Guo LJ. Inter-particle collision effects on the entrained particle distribution in aeolian sand transport. Int J Heat Mass Tran. 2013;58:97–106. doi: 10.1016/j.ijheatmasstransfer.2012.11.029.

[10] Yan WL, Wu G, Dong ZQ. Optimization of the mix proportion for desert sand concrete based on a statistical model. Constr Build Mater. 2019;226:469–82. doi: 10.1016/j.conbuildmat.2019.07.287.

[11] Dong W, Shen XD, Zhao ZB, He J, Yu TT. Study of the freezing-thawing damage and life prediction of aeolian lightweight aggregate concrete. J Glaciol Geocryol. 2015;37(4):1009–15. https://www-webofscience-com-s.webvpn.imust.edu.cn:8118/wos/alldb/full-record/CSCD:5641826.

[12] Al-Harthy AS, Halim MA, Taha R, Al-Jabri KS. The properties of concrete made with fine dune sand. Constr Build Mater. 2007;21(8):1803–8. doi: 10.1016/j.conbuildmat.2006.05.053.

[13] Abu Seif ES, Sonbul AR, Hakami BA, El-Sawy EK. Experimental study on the utilization of dune sands as a construction material in the area between Jeddah and Mecca, Western Saudi Arabia. B Eng Geol Environ. 2016;75(4):1–16. doi: 10.1007/s10064-016-0855-9.

[14] Wu JC, Shen XD, Hao YH. Research and prediction on carbonation of aeolian sand concrete. B Chin Ceram Soc. 2017;36(7):2306–9. https://www-webofscience-com-s.webvpn.imust.edu.cn:8118/wos/alldb/full-record/CSCD:6047236.

[15] Luo FG, He L, Pan Z, Duan WH, Zhao XL. Effect of very fine particles on workability and strength of concrete made with dune sand. Constr Build Mater. 2013;47:131–7. doi: 10.1016/j.conbuildmat.2013.05.005.

[16] Dong ZQ, Wu G, Lian JL. Experimental study on the durability of FRP bars reinforced concrete beams in simulated ocean environment. Sci Eng Compos. 2018;25(6):1123–34. doi: 10.1515/secm-2017-0237.

[17] Sui JH. Study on chloride transport behavior and service performance of cracked lining concrete in Binhai Metro tunnel. Qingdao University of Technology. 2021;52(5):622–32. doi: 10.27263/d.cnki.gqudc.2021.000494.

[18] Chen WK, Liu QF. Numerical study on the coupled transmission of moisture and multi-ions in concrete under alternating wet and dry conditions. J Hydraul Eng. 2021;52(5):622–32. doi: 10.13243/j.cnki.slxb.20201099.

[19] Liu JX, Li N, Chen MR, Yang JP, Long B, Wu ZS. Durability of basalt fiber-reinforced polymer bars in wet-dry cycles alkali-salt corrosion. Sci Eng Compos Mater. 2019;26(1):43–52. doi: 10.1515/secm-2018-0030.

[20] Mangat PS, Molloy BT. Prediction of long term chloride concentration in concrete. Mater Struct. 1994;27(170):338–46. doi: 10.1617/s11527-022-01879-y.

[21] Amey SL, Johnson DA, Miltenberger MA, Farzam H. Predicting the service life of concrete marine structures: an environmental methodology. ACI Struct J. 1998;95(2):205–14. doi: 10.14359/540.

[22] Zhang CL, Chen WK, Mu S, Šavija B. Numerical investigation of external sulfate attack and its effect on chloride binding and diffusion in concrete. Constr Build Mater. 2021;285:122806. doi: 10.1016/j.conbuildmat.2021.122806.

[23] Shi HS, Wang Q. Research on service life prediction of marine concrete. J Build Eng. 2004;2:161–7. doi: 10.3969/j.issn.1007-9629.2004.02.007.

[24] Yu HF, Sun W, Yan LH. Research on the prediction method of concrete service life I-Theoretical model. J Chin Chem Soc. 2002;30(6):686–90. doi: 10.3321/j.issn:0454-5648.2002.06.004.

[25] Kang TB, Liu Y, Zhou JH. Chloride ion transmission performance of waste fiber recycled concrete under dry-wet cycles. J Build Eng. 2022;25(4):389–94. https://www-webofscience-com-s.webvpn.imust.edu.cn:8118/wos/alldb/full-record/CSCD:7228463.

[26] An MZ, Wang H, Wang Y. Durability of reactive powder concrete under freezing and thawing of seawater. China Railway Science. 2018;39(2):1–9. doi: 10.3969/j.issn.1001-4632.2018.02.01.

[27] JGJ55-2011, Specification for mix proportion design of ordinary concrete. National Standards of the People's Republic of China; 2011. https://www.doc88.com/p-9979668431338.html.

[28] JGJ 52-2006, Standard for quality and test methods of sand and stone for ordinary concrete. National Standards of the People's Republic of China; 2006. https://www.doc88.com/p-9979668431338.html.

[29] GB/T 50080-2016, Standard for test methods of performance on ordinary concrete; 2016. https://www.zhulou.net/post/28889.html.

[30] T/CECS 726-2020, Standard of indoor simulated environmental test method for durability of concrete structures. China

Building Industry Press; 2020. http://www.gong123.com/jianzhu/1419778.html.
[31] JTS/T 236-2019, Technical Specifications for Testing and Testing of Concrete in Water Transport Engineering. MOT; 2019. https://max.book118.com/html/2019/0609/6102233141002035.shtm.
[32] Wang CF. Research on the durability of polypropylene fiber concrete in chloride environment. Xi'an: Xi'an University Of Architecture And Technology; 2012. doi: 10.7666/d.d245017.
[33] Xiao Y. Water and chloride ion transport behavior and life prediction of aeolian sand concrete. Baotou: Inner Mongolia University of Science and Technology; 2021. doi: 10.27724/d.cnki.gnmgk.2021.000194.
[34] Wang J, Ng PL, Su H, Du J. Influence of the coupled time and concrete stress effects on instantaneous chloride diffusion coefficient. Constr Build Mater. 2020;237:117645. doi: 10.1016/j.conbuildmat.2019.117645.
[35] Helland S. Assessment and prediction of service life of marine structures-A tool for performance based requirement. Workshop On Design Of Durability Of Concrete; 1999. doi: 10.26914/c.cnkihy.2020.028164.
[36] Chen XD, Zhang Q, Gu X, Li X. Probability analysis on service life prediction of reinforced concrete structures. J Chinese Soc Corros Prot. 2021;41(5):673–8. https://www.semanticscholar.org/paper/PREDICTING-THE-RISK-OF-REINFORCEMENT-CORROSION-IN-Bamforth/70c0233260d1a85d18268b0ac27c9f0945eca88c.
[37] Duracrete PS. General guidelines for durability design and redesign. CUR: The European Union; 2000. https://lib.ugent.be/catalog/rug01:001386862.
[38] Giorv ODDE. Durability design of concrete structure under severe environment. Boca Raton: CRC Press; 2010. https://schlr.cnki.net/Detail/index/GARBLAST/STBD92D5561B8A411DD2E594D59B1E40DBDB.
[39] Wang H. Research on the durability of reactive powder concrete under the action of seawater freeze-thaw cycles. Beijing: Beijing Jiaotong University; 2014. https://kns.cnki.net/KCMS/detail/detail.aspx?dbname=CMFD201402&filename=1014141169.nh.